International Journal of Offshore and Polar Engineering (ISSN 1053-5381)

Vol. 21, No. 3, September 2011, pp. 233–239

http://www.isope.org/publications

Wave-induced Pore Pressure Responses and Soil Liquefaction Around Pile Foundation

Xiao-Jun Li, Fu-Ping Gao* and Bing Yang*
Institute of Mechanics, Chinese Academy of Sciences, Beijing, China

Jun Zang
Department of Architecture & Civil Engineering, University of Bath, Bath, UK

A 3D FEM model is proposed and verified with existing experimental data for simulating wave-induced transient and residual pore pressure responses around a pile foundation. The numerical results show that the residual pore pressure tends to be amplified at the bottom of the pile foundation; near it, this pressure increases and the amplitude of transient pore pressure decreases with the decrease of soil permeability. The wave nonlinearity affects both transient and residual pore pressures around the pile. The effect of the pile diameter on the oscillatory pore pressure is much more obvious than that on the buildup of pore pressure. The liquefaction zone around the pile is asymmetric; the maximum liquefaction depth appears at the back of the pile foundation.

INTRODUCTION

Piles have been widely used for the foundartions of coastal and offshore structures, such as platforms, long-spanning bridges, offshore wind farms, etc. Under the action of ocean waves, pore water pressure may be induced in the seabed around pile foundations, which is usually accompanied by the reduction of effective stresses. In some extreme conditions, such as hurricanes or storms, the soil around the pile foundation may be liquefied, resulting in large displacements of the pile foundation and the eventual collapse of upper structures. Thus, a proper evaluation of wave-induced pore pressure responses and soil liquefaction around the pile foundation is crucial for the geotechnical design of maritime structures.

Generally, there are 2 significant mechanisms for wave-induced pore pressure responses, which are also observed in laboratory experiments and field measurements (i.e., Nago et al., 1993). The first mechanism, termed transient or oscillatory pore pressure, is characterized by the attenuation of amplitude and the phase lag within the seabed. The other is residual buildup of pore pressure caused by the compression of the soil skeleton, which is similar to the pore pressure responses induced by earthquakes.

Since the 1970s, wave-induced pore pressure responses and liquefaction within a porous seabed have gradually concerned marine geotechnical engineers and researchers. Based on the conventional Biot consolidation equations (Biot, 1941), the transient characteristics of excess pore pressure for an infinite seabed have been studied theoretically by Yamamoto et al. (1978). Then, within the same framework, a series of analytical solutions has been accomplished by considering the finite thickness of the seabed and orthotropic nature of soil (Jeng and Hsu, 1996; Jeng, 1997). On the other hand, the residual buildup of pore pressure has been investigated by some researchers (Seed and Rahman, 1978; McDougal et al., 1989; Sumer and Fredsøe, 2002; Jeng et al., 2007). The empirical relationships obtained from dynamic triaxial or simple shear tests have been employed to model the pore pressure generation under an undrained condition (DeAlba et al., 1975; Seed et al., 1976). All this research, however, mainly focused on one of the mechanisms for the pore pressure responses individually. In fact, the wave-induced transient and residual pore pressure responses are coupled.

Numerous studies have also been conducted to investigate the pore pressure responses and soil liquefaction around marine structures. For instance, Rahman et al. (1977) developed a practical procedure to analyze the pore pressure responses and soil liquefaction under the Ekofisk oil tank. Zhou and Qiu (1993) obtained a closed-form analytical solution of wave-induced seepage pressure acting on the base of a breakwater in an infinite-depth elastic seabed. Based on flume experiments, Sumer et al. (1999, 2006) have systematically examined the pore pressure response around the pipeline buried in the soil and sinking/floating of pipelines. A review of pore pressure responses of soil around offshore structures could also be found in Jeng (2003). Recently, Lu and Jeng (2008, 2010), based on the boundary element method (BEM), investigated the seismic wave-induced pile-soil interaction responses. However, the ocean wave-induced pore pressure responses and soil liquefaction around pile foundations have not been well understood.

In this study, a FEM model is proposed to simulate the wave-induced transient and residual pore pressure responses simultaneously around a pile foundation. The numerical model is verified with the existing experimental data from Sumer et al. (1999). The pore pressure responses in the vicinity of the pile foundation have been compared with those in the absence of pile, and the effects of wave nonlinearity have also been investigated. A parametric study is made to examine the influences of soil permeability and pile diameter on transient and residual pore pressure responses near the pile foundation. Finally, the existing criterion of liquefaction is applied to investigate the distribution of liquefied depth around the pile foundation.

NUMERICAL MODEL

The wave-induced pore pressure responses around a pile foundation is investigated in this study, which involves the interaction between wave, soil and pile, as shown in Fig. 1. The profile of the

*ISOPE Member.

Received August 5, 2010; revised manuscript received by the editors January 13, 2011. The original version (prior to the final revised manuscript) was presented at the 20th International Offshore and Polar Engineering Conference (ISOPE-2010), Beijing, June 20–26, 2010.

KEY WORDS: Ocean wave, pile foundation, transient and residual pore pressure, soil liquefaction, FEM.

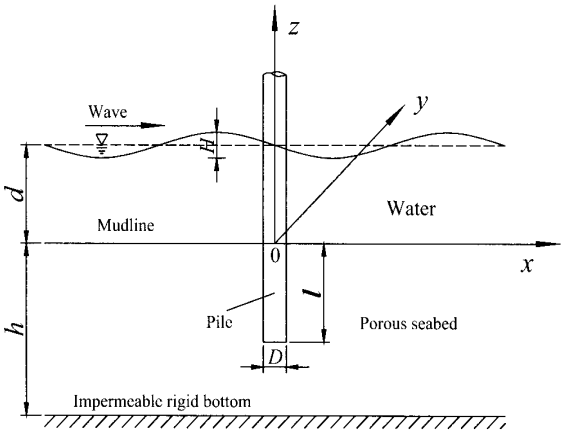

Fig. 1 Definition of wave-seabed-pile interaction problem

pile foundation is characterized by the diameter D and the depth of embedment l. The wave is assumed to propagate in the positive x-direction, while the z-direction is upward from the interface between water and porous seabed.

Governing Equations

According to Darcy's law and the continuity of pore water, the governing equation for the flow of pore water within the seabed can be deduced with the assumptions of compressible pore water and soil skeleton:

$$\frac{k_s}{\gamma_w}\left(\frac{\partial^2 p}{\partial x^2}+\frac{\partial^2 p}{\partial y^2}+\frac{\partial^2 p}{\partial z^2}\right)-\frac{n}{K'}\frac{\partial p}{\partial t}=\frac{\partial \varepsilon}{\partial t} \tag{1}$$

where p is the excess pore pressure, k_s the coefficient of soil permeability, γ_w the unit weight of pore fluid, and n the porosity of soil. It is noted that K' is the apparent bulk modulus of pore water, which is defined by:

$$\frac{1}{K'}=\frac{1}{K}+\frac{1-S_r}{P_{w0}} \tag{2}$$

in which K is the true bulk modulus of elasticity of water (taken as 2×10^9 Pa), S_r is the degree of saturation, and $P_{w0}=\gamma_w d$ is the absolute pressure. (d is the water depth.)

In Eq. 1, ε is the volumetric strain of soil skeleton and the volume reduction is considered positive. According to the analysis by Seed and Rahman (1978) on the soil liquefaction under cyclic loading, there exists a relationship between volume change and the change of effective bulk stress, which corresponds to the dissipation of pore pressure from the soil skeleton for a fully drained condition, that is:

$$\frac{\partial \varepsilon}{\partial t}=m_v\left(\frac{\partial p}{\partial t}-\psi\right) \tag{3}$$

where ψ is regarded as a source term and defined by the rate of pore pressure generation for undrained soil, i.e. $\psi=\partial u_g/\partial t$, in which u_g is the amount of pore pressure generation. For the linear elastic material under the 3D condition, the coefficient of volume compressibility can be written as:

$$m_v=\frac{1-2\mu}{6G(1+\mu)} \tag{4}$$

Substituting Eq. 3 into Eq. 1, we have:

$$\frac{\partial p}{\partial t}=\frac{1}{n/K'+m_v}\left(\frac{k_s}{\gamma_w}\nabla^2 p+m_v\psi\right) \tag{5}$$

To solve the above equation, it is necessary to describe the amount of pore pressure generation u_g in undrained soil. Here it is given by Seed et al. (1976) as:

$$\frac{u_g}{\sigma_0'}=\frac{2}{\pi}\arcsin(N/N_l)^{1/2\theta} \tag{6}$$

in which $\sigma_0'=((1+2K_0)/3)\gamma' z$ is the initial effective normal stress, where K_0 is the coefficient of lateral earth pressure and γ' the submerged specific weight of soil. θ is the empirical constant and its typical value, set by Seed et al. (1976), is 0.7.

Rahman and Jaber (1986) assumed the above nonlinear relationship (Eq. 6) can be simplified as a linear approximation:

$$\frac{u_g}{\sigma_0'}=\frac{N}{N_l} \tag{7}$$

where N_l is the number of shear stress cycles required to cause the initial liquefaction, which is usually related to the cyclic shear stress ratio τ/σ_0', that is:

$$N_l=\left(\frac{1}{\alpha}\frac{\tau}{\sigma_0'}\right)^{1/\beta} \tag{8}$$

in which α and β are empirical constants, determined by the soil type and relative density of soil (McDough et al., 1989) and τ represents the amplitude of cyclic shear stress. In this numerical study, the analytical solution by Jeng and Hsu (1996) is employed to determine the amplitude of cyclic shear stress:

$$\tau=p_0[(C_1-C_2kz)e^{-kz}-(C_3-C_4kz)e^{kz} +k\delta(C_5e^{-\delta z}-C_6e^{\delta z})] \tag{9}$$

where $p_0=\gamma_w H/2\cosh(kd)$ is the amplitude of pressure at the seabed surface induced by linear waves, in which H is the wave height, k the wave number, and d the water depth. C_i ($i=1,\ldots,6$) and δ are parameters closely related to the wave characteristics and soil properties. The details can be found in the paper by Jeng and Hsu (1996). Eq. 9 shows that the amplitude of shear stress τ in the seabed in finite thickness is determined by both wave and soil characteristics. It should be noted that Jeng (2008) extended the above result to consider the 2nd-order nonlinear effects on the residual pore pressure response in marine sediments, which has also been incorporated into the present model to consider the effects of wave nonlinearity on the pore pressure responses around the pile foundation.

Initial and Boundary Conditions

In order to solve the aforementioned governing Eq. 5, the initial and boundary conditions are set as follows:

- At the surface of the seabed ($z=0$), the pore pressure is equal to the surface pressure induced by the 2nd-order Stokes linear progressive waves, that is $p=p_0\cos(kx-\omega t)$, where k is the wave number, ω is the wave frequency, and

$$p_{2\text{nd}}=\frac{\gamma_w kH^2}{8\sinh(2kd)}\left[\left(\frac{3}{\sinh^2(kd)}-1\right)\cos 2(kx-\omega t)-1\right]$$

denotes the 2nd-order component of waves. If neglecting the nonlinear term, the surface pressure reduces to a linear wave problem.

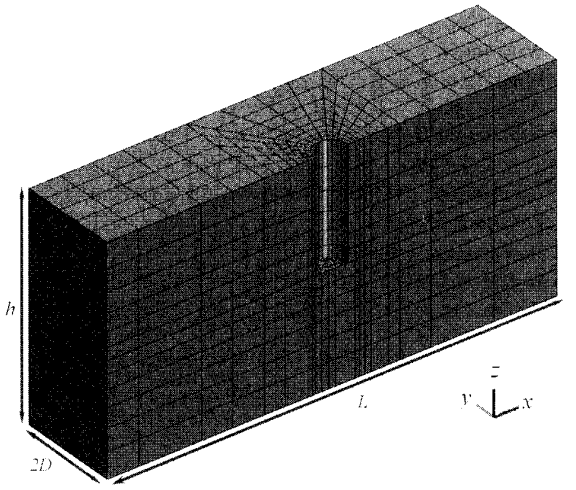

Fig. 2 Sketch of 3D numerical model and FE mesh

• At the bottom of the seabed ($z = -h$) and the interface between soil and pile foundation ($x^2 + y^2 = D^2/4$ or $z = -l$), no flow occurs, i.e. $\partial p/\partial n = 0$.

• A wave length of L in the x-direction is chosen to apply to the periodic-type lateral boundary, which obeys the principle of repeatability (Zienkiewicz and Scott, 1972), that is, $p|_{x=-L/2} = p|_{x=L/2}$.

• According to the symmetric characteristics of linear waves and geometric profile of the pile foundation, the proposed numerical model can be simplified as a 3D symmetric problem in the $x - z$ plane (Fig. 2); thus, the Newman boundary condition $\mathbf{n} \cdot \nabla p = 0$ is used to simulate the symmetric boundary condition at $y = 0$.

Fig. 2 shows the computation domain of the numerical model and the finite element mesh used in this study. Quadratic Lagrange elements are adopted and finer meshes are divided in the vicinity of the pile foundation to ensure the accuracy of numerical modeling. Numerical tests showed that a time step of $T/10$ is necessary to properly simulate both components of transient and residual pore pressure. Meanwhile, the pore pressure distribution is approximately the same around the pile for the width of the calculation zone (in the y-direction) from $1.8D$ up to $2.5D$, indicating the width of $2.0D$ is sufficient to eliminate the boundary effect. Here D is the pile diameter, and h is the thickness of the seabed (Fig. 2).

RESULTS AND DISCUSSIONS

Verification of Numerical Model

To verify this proposed numerical model, the experimental data from Sumer et al. (1999) for the undisturbed-flow case are employed. For comparison, wave and soil parameters used in the numerical model are consistent with those in the experiments by Sumer et al. (1999), as shown in Fig. 3's caption. Fig. 3a illustrates the time development of pore pressure at $z = -0.072$ m. It can be seen from the figure that the 2 mechanisms—transient and residual pore pressures—exist simultaneously. The residual pore pressure increases obviously at the initial stage ($t < 35$ s) and reaches the maximum value at a certain time (e.g. $t = 35$ s in the figure). It then tends to decrease slightly at the last stage. This

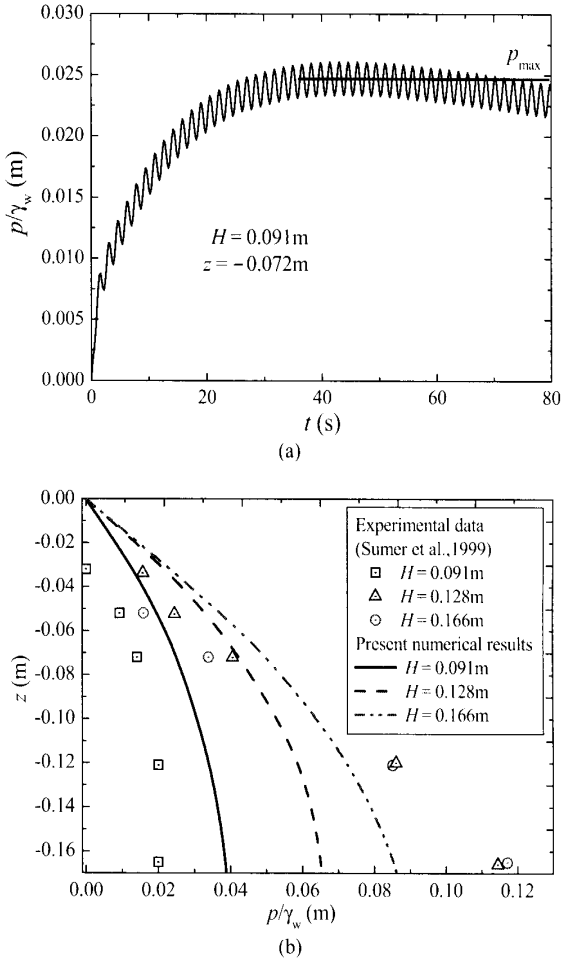

Fig. 3 Comparisons of pore pressure responses between present numerical results and experimental data from Sumer et al. (1999): (a) time development of pore pressure at $z = -0.072$ m; (b) vertical distributions of maximum value of residual pore pressure, where $T = 1.6$ s, $d = 0.42$ m, $L = 2.89$ m, $h = 0.17$ m, $G = 5.4 \times 10^5$ N/m^2, $k_s = 5.37 \times 10^{-8}$ m/s, $\mu = 0.35$, $n = 0.35$, $S_r = 1.0$, $K_0 = 0.41$, $\alpha = 0.48$, $\beta = -0.29$

pattern is in accordance with the physical observations by Sumer et al. (1999). Fig. 3b shows comparisons of vertical distributions of the maximum value (p_{max}) of residual pore pressure within the soil between the present numerical results and the experimental data from Sumer et al. (1999). It is indicated that the tendency for the numerical results—i.e. p_{max} increases with the increment of soil depth—is the same as that for the experimental measurements, although there exist some differences between them for the maximum value of residual pore pressure.

Comparisons of Pore Pressure Responses Between Vicinity of Pile Foundation and Seabed Without Pile

In this study, the pore pressure responses in the vicinity of pile foundations are investigated. Meanwhile, the corresponding results within the seabed in the absence of pile are also obtained for comparisons. Table 1 lists the parameters for the numerical modeling.

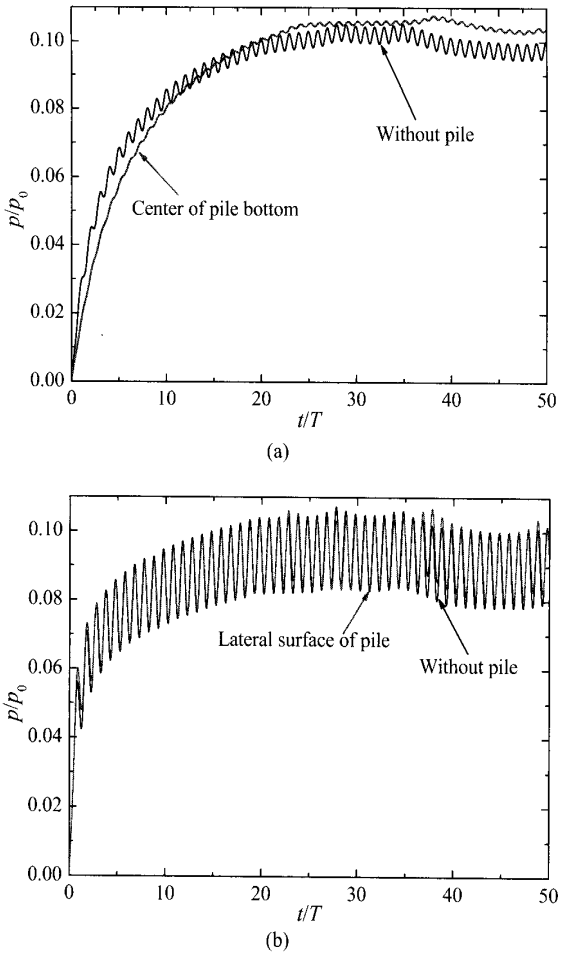

Fig. 4 Time developments of pore pressures in vicinity of pile foundation and within seabed without pile: (a) center of pile bottom at (0, 0, $-l$); (b) lateral surface of pile at ($D/2$, 0, $-3l/4$), where $D = 6.0$ m, $l = 12.0$ m

Fig. 4 shows the time developments of pore pressures at the center of the pile bottom and at the lateral surface of the pile foundation. The corresponding results in the seabed without pile are presented in the figure for comparison. It is seen from Fig. 4a that the residual component of pore pressure seems to be amplified due to the existence of the pile foundation, while the amplitude of transient pore pressure is reduced. On the other hand, there are little differences for the variations of pore pressure with the time at the lateral position of the pile foundation, compared with those in the seabed without pile (Fig. 4b). It is noted that the existence of pile has obvious influences on the distributions of pore pressure in the vicinity of the pile bottom, but little effects on those at the pile's lateral position.

Effects of Wave Nonlinearity on Pore Pressure Responses Around Pile Foundation

Based on the nonlinear wave theory (Dean and Dalrymple, 1991), Jeng (2008) deduced the analytical solution of the 2nd-order wave-induced pore pressure at the seabed surface ($z = 0$) and the shear stress amplitude within the seabed, both of which have been incorporated into the present numerical model to investigate the influences of wave nonlinearity on the pore pressure responses around the pile foundation. The values listed in Table 1 have also been employed as the input data in this section.

Wave characteristics	
Wave period T	6.0 s
Water depth d	15.0 m
Wave length L	53.0 m
Wave height H	5.0 m
Pile characteristics	
Diameter D	6.0 m (various)
Embedded depth$l$	12.0 m
Seabed characteristics	
Seabed thickness h	24.0 m
Poisson's ratio μ	0.35
Soil porosity n	0.46
Shear modulus G	1.5×10^7 N/m^2
Permeability k_s	1.0×10^{-4} m/s (various)
Unit weight of pore water γ_w	9.8×10^3 N/m^3
Submerged specific weight of soil γ'	10.73×10^3 N/m^3
Degree of saturation S_r	1.0
Coefficient of lateral earth pressure K_0	0.41
α	0.25 (various)
β	−0.29 (various)

Table 1 Input data for present numerical study

Fig. 5 illustrates the pore pressure responses around the pile foundation under linear and nonlinear waves. As shown in Fig. 5a, it can be seen that the 2nd-order component of waves has some influences on both transient and residual pore pressure responses near the pile foundation, e.g. at the lateral position of ($D/2$, 0, $-l/4$) where the transient pressure dominates, the nonlinear wave-induced pore pressure is somewhat amplified, and the residual pore pressure induced by nonlinear waves is slightly less than that of linear waves at the centre point of the foundation bottom. Fig. 5b shows the distributions of pore pressure responses along the lateral surface of the pile foundation at the different characteristic time when wave crests pass the pile, e.g. $t/T = 1$, 5, 10, separately. There exist some differences between the linear and the 2nd-order Stokes nonlinear wave-induced pore pressures along the lateral surface of the pile foundation.

Parametric Study

A parametric study is carried out here to examine the influences of soil permeability k_s and pile diameter D on both transient and residual pore pressure responses around the pile foundation. Note: The results below are for the case of linear wave loading. The other parameters for wave, soil and the pile used here remained the same as shown in Table 1.

Fig. 6 presents the time developments of pore pressure at the center of the pile's bottom and the vertical distributions of pore pressure along the lateral surface of the pile foundation with different values of soil permeability k_s. As shown in Fig. 6a, for $k_s = 1.0 \times 10^{-3}$ m/s, the residual pore pressure is not induced and the oscillatory component prevails. On the other hand, for $k = 1.0 \times 10^{-5}$ m/s, the buildup of pore pressure gets much more obvious. The figure also shows that pore pressure buildup increases gradually with the decrease of soil permeability. Plus, the duration period for the pore pressure buildup to its maximum value decreases with the increase of soil permeability. Fig. 6b illustrates the vertical distributions of pore pressures along the lateral surface of the pile foundation. All of them correspond to the

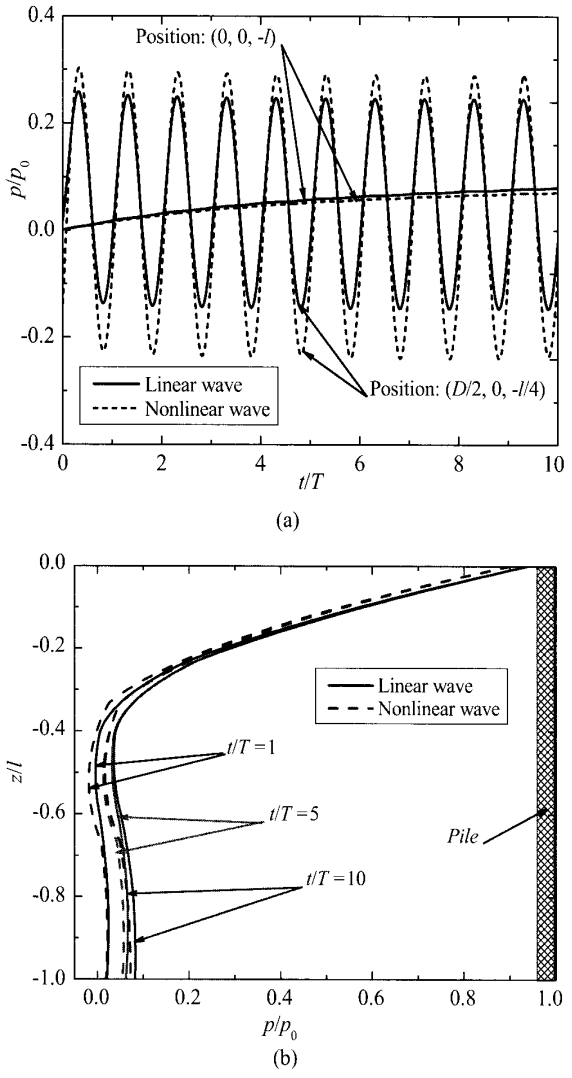

Fig. 5 Comparisons of pore pressure responses induced by linear and nonlinear waves around pile foundation: (a) time developments of pore pressures at bottom of pile (0, 0, $-l$) and at lateral surface ($D/2$, 0, $-l/4$); (b) vertical distributions of pore pressures along lateral surface of pile at different time, where $D = 6.0$ m, $l = 12.0$ m

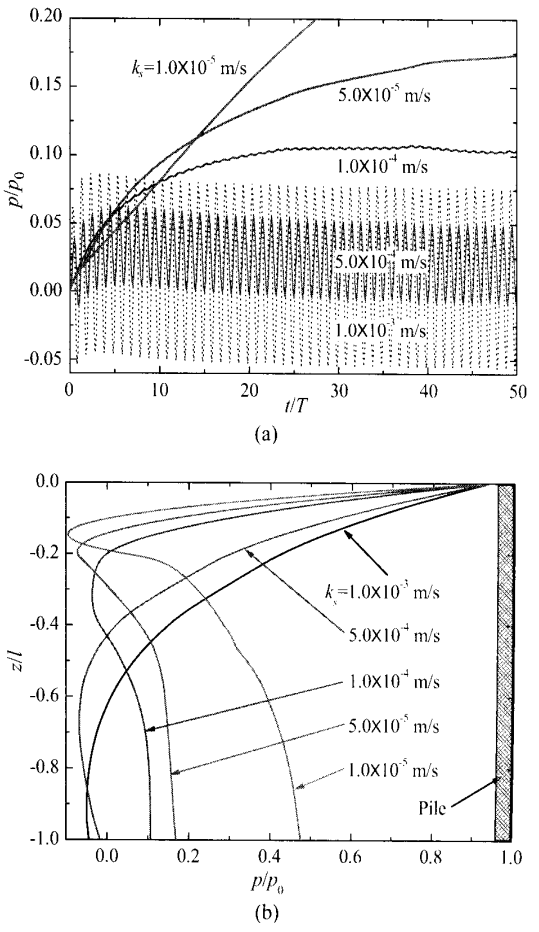

Fig. 6 Variations of pore pressure with changes of soil permeability: (a) time developments of pore pressure at center of pile bottom (0, 0, $-l$); (b) vertical distributions of pore pressure along lateral surface of pile, where $D = 6.0$ m, $l = 12.0$ m

time when the pore pressure reaches the maximum at the position of the pile bottom. It can be seen that the attenuations of pore pressure are significant for all the cases in the upper half of the pile, which may be due to the damping of amplitude and phase lag for the transient pore pressure within the seabed. Further, the rate of the pore pressure attenuation is more obvious for smaller soil permeability; for the lower half of the pile, in which the transient component seems to decay to zero, the component of residual pore pressure becomes dominant and its value increases with the decrease of soil permeability.

Fig. 7 shows the time developments of pore pressure at the center of the bottom of pile foundations and vertical distributions of pore pressure along the lateral surface of pile foundations with various pile diameters D. As shown in Fig. 7a, the pile foundation's diameter has influence on the amplitude of transient pore pressure at the bottom of the pile, decreasing with the increase of pile diameter. However, the value and rate of pore pressure buildup and dissipation are not very sensitive to the pile diameter. The reasons could be as follows:

- The pile foundation's diameter is small relative to the wave length L; here $D/L \approx 0.038$, 0.075, 0.11 separately.
- The residual pore pressure has sufficient time to diffuse or spread within the seabed because of its larger time0scale relative to the oscillatory pore pressure.

Fig. 7b shows the vertical distributions of pore pressure along the lateral surface of the pile foundation at the moment when pore pressure arrives at the maximum at the pile bottom. It is indicated that the larger the pile diameter, the faster the pore pressure attenuates for the pile's upper half, while at the pile foundation's lower half, the pore pressure, especially for the residual component, is not sensitive to the pile diameter.

Soil Liquefaction Around Pile Foundation

When the pore pressure variation between the seabed surface and a certain depth equals to or exceeds the overburden soil pressure, the soil reaches the state of momentary liquefaction. The criterion for momentary liquefaction can be expressed as:

$$(p - p_{bed}) + \frac{1}{3}(1 + 2K_0)\gamma' z \geq 0 \tag{10}$$

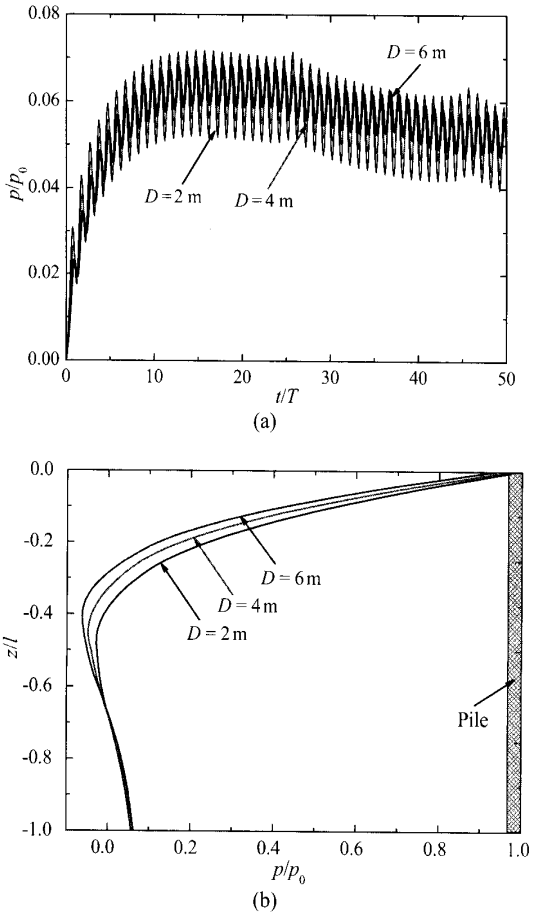

Fig. 7 Pore pressure variations with changes of pile diameter: (a) time developments of pore pressure at center of bottom of pile (0, 0, $-l$); (b) vertical distributions of pore pressure along lateral surface of pile, where $l = 12.0$ m, $k_s = 2.0 \times 10^{-4}$ m/s

in which K_0 is the coefficient of lateral earth pressure and γ' is the submerged specific weight of soil. $(p - p_{bed})$ denotes the differences of pore pressure within the seabed and at the mudline, which contain the effects of both transient and residual pore pressures.

Fig. 8 shows the time development of the liquefied zone around the pile foundation, where $\alpha = 0.1$, $\beta = -0.35$, $T = 6.0$ s, $D = 6.0$ m, $l = 12.0$ m, respectively. Here a typical time of a half-wave period when wave troughs pass the pile center is chosen to analyze the distributions of the liquefied depth near the pile. It is implied that the distributions of the liquefaction zone around the pile foundation are asymmetric for the phase lag of momentary pore pressure (Fig. 8a, b). Meanwhile, owning to the pore pressure accumulation, the soil liquefaction expands gradually and finally attends maximum value. The maximum depth of liquefaction appears at the back of the pile foundation at the typical time (Fig. 8b).

CONCLUSIONS

A FEM model is presented to simulate both residual and oscillatory pore pressure responses simultaneously around the pile foundation, which is verified with the existing experimental data.

It is indicated that the residual pore pressure response is amplified at the bottom of the pile foundation, while the amplitude of

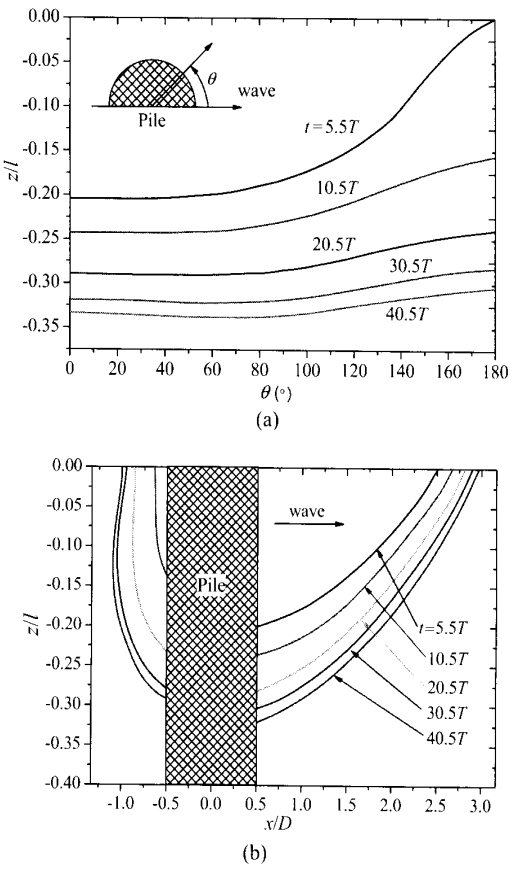

Fig. 8 Time development of liquefied zone around pile foundation: (a) along circumferential direction; (b) at symmetric face, where $\alpha = 0.1$, $\beta = -0.35$, $T = 6.0$ s, $D = 6.0$ m, $l = 12.0$ m

transient pore pressure at the same location decreases obviously, compared with that in the seabed without pile. Meanwhile, the effects of wave nonlinearity on both transient and residual pore pressures around the pile foundation are significant.

With the decrease of soil permeability, the residual component of pore pressure increases significantly and the amplitude of oscillating pore pressure diminishes. The effect of the pile diameter on the oscillatory pore pressure is much more obvious than that on the build-up of residual pore pressure.

Existence of residual pore pressure tends to exacerbate the possibility of transient liquefaction in the seabed. The liquefied zone around the pile foundation is asymmetric in nature, and the maximum depth of soil liquefaction appears at the back of the pile foundation at the typical time of half wave period.

ACKNOWLEDGEMENTS

This work is financially supported by the National Natural Science Foundation of China (Grant No. 10872198) and the Knowledge Innovation Program of the Chinese Academy of Sciences (KJCX2-YW-L07).

REFERENCES

Biot, MA (1941). "General Theory of Three-dimensional Consolidation," *J Appl Phys*, Vol 12, pp 155–164.

DeAlba, P, Chan, CK, and Seed, HB (1975). "Determination of Soil Liquefaction Characteristics by Large-Scale Laboratory

Tests," *Rept No EERC 75-14*, Earthquake Eng Res Center, Univ of California, Berkeley.

Dean, RG, and Dalrymple, RA (1991). *Water Wave Mechanics for Engineers and Scientists*, World Scientific, Singapore.

Jeng, DS, and Hsu, JRC (1996). "Wave-induced Soil Response in a Nearly Saturated Seabed of Finite Thickness," *Géotechnique*, Vol 46, pp 427–440.

Jeng, DS (1997). "Wave-induced Seabed Instability in Front of a Break-water," *Ocean Eng*, Vol 24, pp 887–917.

Jeng, DS (2003). "Wave-induced Seafloor Dynamics," *Appl Mech Rev*, Vol 56, No 4, pp 407–429.

Jeng, DS, Seymour, B, Gao, FP, and Wu, YX (2007). "Ocean Waves Propagating over a Porous Seabed: Residual and Oscillatory Mechanisms," *Sci in China, Series E Tech Sciences*, Vol 50, No 1, pp 81–89.

Jeng, DS (2008). "Effects of Wave Non-Linearity on Residual Pore Pressure in Marine Sediments," *The Open Civil Eng Journal*, Vol 2, pp 63–74.

Lu, JF, and Jeng, DS (2008). "Poroelastic Model for Pile-Soil Interaction in a Half-Space Porous Medium Due to Seismic Waves," *Int J Numer and Analyt Meth in Geomech*, Vol 32, No 1, pp 1–41.

Lu, JF, and Jeng, DS (2010). "Dynamic Response of Offshore Pile to Pseudo-Stoneley Waves Along Interface Between Poroelastic Seabed and Seawater," *Soil Dyn and Earthquake Eng*, Vol 30, No 4, pp 184–201.

McDougal, WG, Tsai, YT, Liu, PL-F, and Clukey, EC (1989). "Wave-induced Pore Water Pressure Accumulation in Marine Soils," *J Offshore Mech and Arctic Eng*, Vol 111, pp 1–11.

Nago, H, Maeno, S, Matsumoto, T, and Hachiman, Y (1993). "Liquefaction and Densification of Loosely Deposited Sand Bed Under Water Pressure Variation," *Proc 3rd Int Offshore and Polar Eng Conf*, Singapore, ISOPE, Vol 1, pp 578–584.

Rahman, MS, Seed, HB, and Brook, JR (1977). "Pore Pressure Development Under Offshore Gravity Structures," *J Geotech Eng Div*, ASCE, Vol 103 (GT 12), pp 1419–1437.

Rahman, MS, and Jaber, WY (1986). "A Simplified Drained Analysis for Wave-induced Liquefaction in Ocean Floor Sands," *Soils and Found*, Vol 26, No 3, pp 57–68.

Seed, HB, Martin, PQ, and Lysmer, J (1976). "Pore-water Pressure Changes During Soil Liquefaction,"*J Geotech Eng Div*, ASCE, Vol 102 (GT 4), pp 323–346.

Seed, HB, and Rahman, MS (1978). "Wave-induced Pore Pressure in Relation to Ocean Floor Stability of Cohesionless Soils," *Marine Geo-tech*, Vol 3, No 2, pp 123–150.

Sumer, BM, Fredsøe, J, Christensen, S, and Lind, MT (1999). "Sinking/Floatation of Pipelines and Other Objects in Liquefied Soil Under Waves," *Coastal Eng*, Vol 38, No 2, pp 53–90.

Sumer, BM, and Fredsøe, J (2002). *The Mechanics of Scour in the Marine Environment*, World Scientific, Singapore.

Sumer, BM, Truelsen, C, and Fredsøe, J (2006). "Liquefaction Around Pipelines Under Waves," *J Waterway Port Coastal and Ocean Eng*, ASCE, Vol 132, No 4, pp 266–275.

Yamamoto, T, Koning, H, Sellnejjer, H, and Van Hijum, E (1978). "On the Response of a Poroelastic Bed to Water Waves," *J Fluid Mech*, Vol 87, pp 193–206.

Zhou, ZL, and Qiu, DH (1993). "Analytical Solution of Wave-induced Seepage Pressure Acting on the Base of Breakwater," *J Hydrodyn*, Series B, Vol 5, No 2, pp 42–51.

Zienkiewicz, OC, and Scott, FC (1972). "On the Principle of Repeatability and Its Application in Analysis of Turbine and Pump Impellers," *Int J Numer Meth in Eng*, Vol 9, pp 445–448.